ORIGINAL RESEARCH ARTICLE

WILEY _Journal of_ Cellular Physiology

A negative feedback loop of H19/miR-675/EGR1 is involved in diabetic nephropathy by downregulating the expression of the vitamin D receptor

WenXing Fan[1,2] | YunZhu Peng[3] | Zhang Liang[4] | YueNa Yang[5] | Jing Zhang[1]

[1]Department of Nephrology, the First Affiliated Hospital of Kunming Medical University, Kunming, Yunnan, China

[2]Yunnan Key Laboratory of Laboratory Medicine, the First Affiliated Hospital of Kunming Medical University, Kunming, Yunnan, China

[3]Department of Cardiology, the First Affiliated Hospital of Kunming Medical University, Kunming, Yunnan, China

[4]Department of Science and Technology, Kunming Medical University, Kunming, Yunnan, China

[5]Teaching Quality Monitoring and Assessment Center, Kunming Medical University, Kunming, Yunnan, China

Correspondence
YunZhu Peng, Department of Cardiology, the First Affiliated Hospital of Kunming Medical University, No. 295, Xichang Road, Kunming, 650032 Yunnan, China.
Email: dbnppyz@yeah.net

Abstract

Aim: We aimed to explore the regulatory relationship among the long noncoding RNA H19, micorRNA-675 (miR-675), the vitamin D (VD) receptor (VDR), and the early growth response protein 1 (EGR1) in the pathogenesis of diabetic nephropathy (DN) among patients with diabetes mellitus (DM).

Methods: Expression levels of H19, miR-675, VDR, and EGR in patients or CIHP-1/HEK 293 cells were measured via quantitative reverse-transcription polymerase chain reaction and western blot analysis. Computational analysis and luciferase assays were performed to determine EGR1 as a target gene of miR-675.

Results: The relative expression of miR-675 was higher in the presence of H19, whereas the expression of both VDR and EGR1 messenger RNA was decreased in the presence of H19 or miR-675. However, relative expression of H19 and miR-675 was increased, whereas VDR expression was suppressed upon the treatment of 1,25-dihydroxyvitamin D3 or EGR1. VDR was identified as a target gene of miR-675. The H19 promoter and EGR1 increased the luciferase activity of cells transfected with wild-type VDR. Compared with DM patients free of DN, the levels of H19 and miR-675 were increased in the DN(+) group, whereas the levels of VDR and EGR1 were decreased.

Conclusion: In summary, the above results indicate the presence of a negative feedback loop in the pathological mechanism of DN, where H19 downregulates the expression of VDR by upregulating the expression of miR-675, whereas reduced VDR expression subsequently reduced the expression of EGR1. Moreover, reduced EGR1 expression inhibits H19 expression, thus forming a negative feedback loop required to maintain the homeostasis of VDR and to reduce the incidence of DN.

KEYWORDS
diabetic nephropathy, EGR1, H19, miR-675, VDR

1 | INTRODUCTION

As one of the most common causes of late-stage renal disease, diabetic nephropathy (DN) is associated with a high rate of disability and mortality. Based on a survey conducted by the World Health Organization, it is estimated that 370 million patients will suffer from diabetes in 2030 (Wild, Roglic, Green, Sicree, & King, 2004). It was also reported that approximately 40% of diabetic patients would eventually develop DN in their lifetime (Remuzzi, Schieppati, & Ruggenenti, 2002). The loss of podocytes has become a major mechanism underlying the onset of DN. In fact, podocyte apoptosis has become the earliest cellular disorder affecting the health of diabetic kidneys (Allen, Harwood, Varagunam, Raftery, & Yaqoob, 2003). Previous articles also demonstrated that various pathways are

involved in podocyte apoptosis such as p38 mitogen-activated protein kinase (MAPK), transforming growth factor β, and Notch pathways (G. Li et al., 2013; Tanaka et al., 2014). DN is a common diabetic complication which deteriorates the prognosis of late-stage renal disease (Lippert, Ritz, Schwarzbeck, & Schneider, 1995). Due to glomerular dysfunction, DN is featured by an elevated level of protein leakage into the urine (Friedman, Jones, Golbetz, Lee, & Little, 1983), and glomerular epithelial cells, which are also named podocytes, are a major structural component in the glomerulus. Therefore, the apoptosis of podocytes is reported to lead to the progression of glomerular disorder (Menini et al., 2007).

The H19 gene is found on chromosomes 7 and 11 in the mouse and human, respectively. In these two species, H19 can only be expressed from the maternal allele (Bartolomei, Zemel, & Tilghman, 1991). It has previously been demonstrated that the exon1 of H19 encodes two microRNAs: miR-675-5p and miR-675-3p (Cai & Cullen, 2007). In a previous study, the long noncoding RNA (lncRNA) profiling in VDR$^{-/-}$ mice demonstrated that H19 may participate in the function of VDR signaling during the progression of epidermal disease (Jiang & Bikle, 2014). In fact, H19 was shown to act as a regulator in several pathways. In particular, through miR-675-5p, H19 was shown to regulate the expression of multiple proteins such as runt-related transcription factor, casitas B-lineage lymphoma b (Cbl-b), and retinoblastoma (Tsang et al., 2010). It has also been hypothesized that VDR signaling could inhibit H19 expression by regulating the function of the Mad-1/C-Myc network. Interestingly, H19 could also inhibit VDR expression via miR-675-5p (Chen et al., 2017).

The vitamin D (VD) receptor (VDR) is a transcription factor activated by ligands. Upon its activation, cofactor molecules are recruited to bind at specific DNA locations thus modifying the expression of its target genes (Valdivielso, 2009). It has been shown that VDR can modulate glomerular injury. Interestingly, as an endogenous ligand to VDR, calcitriol can decrease the urinary albumin excretion and glomerulosclerosis index in rats undergoing subtotal nephrectomy (Kuhlmann et al., 2004). In addition, mice with VDR knockout are more prone to develop renal injury during hyperglycemia (Zhang, Sun, et al., 2008). In fact, a combination of VDR activators and angiotensin-converting enzyme (ACE) inhibitors was shown to protect mice against DN Zhang, Zhang, et al., 2008. In the past, numerous reports have demonstrated that merely 2% of the mammalian genome contains gene-coding proteins. Given the fact that many genes in humans are transcribed as noncoding RNAs, this finding is particularly interesting (Ronnau, Verhaegh, Luna-Velez, & Schalken, 2014). lncRNAs are transcripts longer than 200 nucleotides that do not have protein-coding capability. lncRNAs occupy a large portion in the mammalian transcriptome (Perkel, 2013). However, it remains controversial as to whether these lncRNAs are involved in critical cellular processes or whether they are only transcriptional noises (Clark et al., 2011). Unlike lncRNAs, microRNAs (miRNAs) are only 19–22 nucleotides in length that can act as regulators of gene expression (Moreno-Moya, Vilella, & Simon, 2014). The mutual regulation between miRNAs and lncRNAs has aroused much interest these days. In fact, lncRNAs have been found to function as miRNA "sponges." In addition, lncRNAs are shown to behave like competing endogenous RNAs (ceRNAs; Salmena, Poliseno, Tay, Kats, & Pandolfi, 2011). Interestingly, ceRNAs share the same miRNA-binding sites with messenger RNSs (mRNAs) and hence can compete with mRNAs for the binding to miRNAs. In this way, ceRNAs can also control the expression of their target mRNA.

As an active form and a metabolite of vitamin D$_3$, 1,25-dihydroxyvitamin D3 (1,25D3) can bind to VDR. It has been demonstrated previously that the treatment of HL60 cells using 1,25D$_3$ could increase the expression of Egr1 (Danilenko, Wang, & Studzinski, 2001). It has also been shown that miR-675 plays a beneficial role during liver tumorigenesis by regulating the miR-675-HP1α (heterochromatin protein 1α)/EGR1/H19/PKM2 (pyruvate kinase isozymes M1) signaling (Zhang et al., 2008). It has also been reported that the increased expression of H-Ras, PKM2, EGR1, HP1α, lncRNA H19, and miR-675 in patients with liver tumors was accompanied by the increased expression of H19 induced by the early growth response protein 1 (EGR1) signaling (Dey, Pfeifer, & Dutta, 2014). It was suggested that miR-675 and EGR1 could regulate the expression of the H19 promoter through different pathways. In contrast, it was also suggested that EGR1 could enhance the expression of miR-675 by promoting the transcription of H19 (Dey et al., 2014).

H19 is functionally involved in kidney development, whereas miR-675 is located within the chromosome segment of H19 (Dey et al., 2014; X. Li et al., 2016). The increased expression of H19 can increase the expression of both miR-675-5p and miR-675-3p (Dey et al., 2014). Furthermore, VDR was reported as a target gene of miR-675 in human cells, and the activation of the VD signaling pathway could enhance the expression of EGR1, a transcription factor of H19 (Jensen, Yourish, Bunaciu, Varner, & Yen, 2015; H. Li et al., 2015). Based on these results, we hypothesized that H19/miR-675/VDR/EGR1 can form a negative feedback loop to maintain the homeostasis of VDR. When this negative feedback loop is disturbed, it can lead to the development of DN.

2 | MATERIALS AND METHODS

2.1 | Human subject sample collection

This study enrolled 54 DM patients, who were divided into two groups based on the presence of DN: a DN (+) group ($N = 29$) and a DN (−) group ($N = 25$). Samples of renal tissues were collected from all participants. All samples were confirmed by pathological diagnosis and the patients had not received any treatment before the procedure. The clinical and biochemical characteristics of DN(+) patients and DN(−) patients are displayed in Table 1. This study was approved by the Ethics Committee of our institution, and all patients were informed, agreed, and signed the informed consent.

2.2 | RNA isolation and real-time polymerase chain reaction (PCR)

An miRNeasy Mini Kit (Qiagen, Hilden, Germany) was used to extract the total RNA from tissue and cell samples. The expression of H19, miR-675, VDR mRNA, and EGR1 mRNA was measured using quantitative real-time polymerase chain reaction (qRT-PCR) and a

TABLE 1 Clinical and biochemical characteristics of DN(+) and DN(−) patients

	DN(+) patients	DN(−) patients	P value
Gender			
Male	18	14	0.673
Female	11	11	
Age (years)	58 ± 6.3	55 ± 8.7	0.542
Years since diagnosis of DM	8.32 ± 1.32	9.12 ± 2.09	0.602

SYBR® Premix Ex Taq™ II reagent kit (Takara, Dalian, China), following the instructions for the kit. The reaction system volume was 20 μl, including 10.0 μl of One Step SYBR® RT-PCR Buffer III, 0.4 μl of TaKaRa Ex Taq™ HS, 0.4 μl of Prime Script™ RT Enzyme MixII, 0.3 μl of PCR forward: primer, 0.3 μl of PCR reverse: primer, 0.4 μl of ROX reference dye or dye II (50×), 2 μl of total RNA and 6.2 μl of RNase-free ddH$_2$O. An ABI7500 quantitative PCR instrument (ABI Company, Oyster Bay, NY) was used to conduct qRT-PCR. The reaction conditions were as follows: predenaturation at 95°C for 10 s; 40 cycles of denaturation at 95°C for 5 s, annealing and final extension at 60°C for 26 s. U6 was used as the internal reference, and the $2^{-\Delta\Delta C_t}$ method was adopted to calculate the relative expression of H19, miR-675, VDR mRNA, and EGR1 mRNA.

2.3 | Cell culture and transfection

CIHP-1 and HEK 293 cells were cultured in a Dulbecco's modified Eagle's medium containing 10% fetal bovine serum, at a temperature of 37°C, and in an environment of 5% CO$_2$ and saturated humidity. To study the effect of Vitamin D$_3$ on the expression of H19, miR-675, VDR, and EGR1, the cells were cultured in the presence and absence of vitamin D$_3$ before the expression of the above genes was measured.

During cell transfection, the cells were seeded into 24-well plates and transfected using Lipofectamine 2000 (Invitrogen, Carlsbad, CA) following the manufacturer's protocol. The cells were collected at 48 hr posttransfection to measure the expression of target genes. Each experiment was repeated three times.

2.4 | Vector construction and mutagenesis

The fragment sequences of H19, miR-675, and EGR1 were cloned into pcDNA vectors (Promega, Madison, WI), respectively. Subsequently, site-directed mutagenesis was carried out to generate a mutant VDR, which was also cloned into the pcDNA vector for subsequent transfection experiments (see above).

At 48 hr posttransfection, the cells were collected and the luciferase activity of the transfected cells was measured by a microplate reader (Glomax 20/20; Promega) using a dual-luciferase assay system (Promega) following the instruction of the kit manufacturer. A *Renilla* luciferase reporter plasmid (pRL-TK; Promega) expressing *Renilla* luciferase was used as the internal reference of the luciferase assay. Each experiment was repeated three times.

2.5 | Western blot analysis

A total protein extraction rapid immunofilter paper assay kit (Beyotime Biotechnology, Shanghai, China) was used to extract total protein from tissue and cell samples. A bicinchoninic acid assay kit (Beyotime Biotechnology) was then used to determine the protein concentration in the lysate. After resolving the proteins by polyacrylamide gel electrophoresis, the proteins were transferred onto a nitrocellulose membrane by wet transfer. Subsequently, the membrane was blocked in 5% bovine serum albumin for 1 hr at room temperature. Then, the membrane was incubated at 4°C overnight with diluted anti-VDR and anti-EGR1 monoclonal primary antibodies (ab3508 and ab55160; Abcam, Cambridge, MA), washed with phosphate-buffered saline (PBS), and incubated with horserasdish peroxidase (HRP)-labeled immunoglobulin G secondary antibody (Abcam) for 1 hr at room temperature. The membrane was then developed in an enhanced chemiluminescence solution (Pierce, Rockford, IL). Finally, the images of the membrane were captured in a dark room. A semiquantitative method was used to measure the relative expression of target proteins using the following formula: relative expression of target protein = grayscale of target protein band/grayscale of internal reference protein band. The protein band of glyceraldehyde 3-phosphate dehydrogenase was used as the internal reference. The gray value of the target band was analyzed by using ImageJ software (National Institutes of Health, Bethesda, MD).

2.6 | Apoptosis analysis

After 48 hr of transfection, the cells were collected and washed three times with cold PBS, followed by centrifugation to discard the supernatant. The collected cells were then resuspended with PBS to adjust the cell density to 1×10^5/ml. In the next step, 1 ml of precooled 75% ethanol was used to fix the cells at 4°C for 1 hr. Subsequently, 100 μl of RNase was added into each tube in the dark and incubated at 37°C for 30 min. According to the instructions of an annexin-V-fluorescein isothiocyanate (annexin-V-FITC) cell apoptosis detection kit (Sigma-Aldrich, St. Louis, MO), the cells were then stained with annexin-V-FITC, propidium iodide (PI), and 4-(2-hydroxyethyl)-1-piperazineethanesulfonic acid buffer solutions at room temperature for 15 min. Excitation light at a wavelength of 488 nm was used to excite the cells, and the emission light was detected at the wavelengths of 525 nm and 620 nm. A scattered light and band-pass filter was used to detect the signals of FITC and PI fluorescence and to evaluate the apoptotic profiles of the cells. The experiment was repeated three times to calculate the mean values.

2.7 | Immunohistochemistry (IHC)

All specimens were fixed in 10% formalin, embedded with paraffin, sliced to 4-μm serial sections, dewaxed with xylene, rehydrated with alcohol, and the activity of endogenous peroxidase was inactivated with 3% hydrogen peroxide. In the next step, anti-VDR and anti-EGR1 primary antibodies were added (diluted to 1:100; Abcam) for

1 hr of incubation at 37°C, followed by the addition of HRP-labeled secondary antibodies. After being incubated for 30 min in 37°C, a 3,3'-diaminobenzidine substrate solution was added onto the samples dropwise and incubated for 1–2 min. Subsequently, the samples were rinsed with PBS, stained for 1 min using hematoxylin, dehydrated, and mounted in neutral gum for observation.

2.8 | Statistical analysis

The data were analyzed using SPSS 21.0 statistical software. Measurement data were presented using mean ± standard deviations ($\bar{X} \pm SD$). The comparison between two groups was done with t tests. A $p < 0.05$ indicated the difference was statistically significant.

3 | RESULTS

3.1 | H19, miR-675, VDR, and EGR formed a negative feedback loop

To validate the negative feedback loop formed by H19, miR-675, VDR, and EGR, and qRT-PCR and western blot analysis were performed using CIHP-1 and HEK 293 cells transfected with vectors carrying H19 segments or miR-675 segments. As shown in Figure 1a, the relative expression of miR-675 in CIHP-1 cells transfected with H19 or miR-675 was significantly increased compared with that in cells transfected with the negative control. However, the levels of VDR mRNA (Figure 1b) and EGR1 mRNA (Figure 1c) were apparently decreased upon the transfection of H19 or miR-675. Moreover, the western blot analysis also showed consistent results (Figure 1d). Finally, similar results were observed in HEK 293 cells (Figure 1e–h), indicating the upregulation of H19 and miR-675 could lead to reduced expression of VDR and EGR1.

3.2 | Effect of 1,25D$_3$/EGR1 on the H19 signaling pathway

Subsequently, the relative expression of H19, miR-675, and VDR was measured by qRT-PCR and western blot analysis. As shown in Figure 2 and compared with the negative controls, the relative expression of H19 was upregulated in CIHP-1 cells treated with 1,25D$_3$ or EGR1 (Figure 2a). Similarly, miR-675 expression was also increased in the above groups (Figure 2b). However, VDR mRNA and protein were obviously downregulated in the 1,25D$_3$ and EGR1 treatment groups (Figure 2c,d). Finally, similar results were observed in HEK 293 cells subjected to the same treatments (Figure 2e–h). Collectively, the above results established a potential negative feedback loop among H19, miR-675, VDR, and EGR1.

3.3 | VDR was a target gene of miR-675

According to a computational analysis aiming to find the potential target genes of miR-675, a complementary sequence of miR-675-5p was located in the 3′ untranslated region of VDR, indicating that VDR
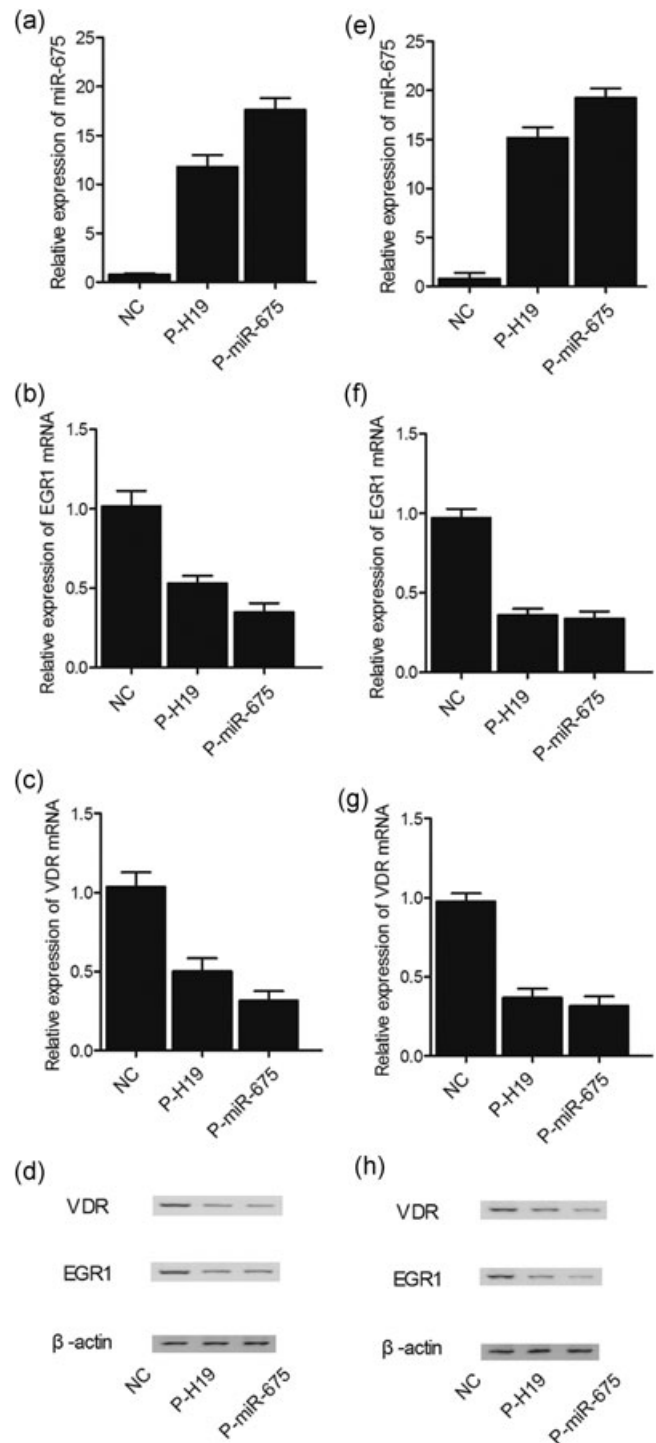

FIGURE 1 Expression levels of miR-675, VDR, and EGR1 in CIHP-1 cells and HEK 293 cells treated with H19 or miR-675; (a) Relative expression of miR-675 in CIHP-1 cells; (b) relative expression of VDR mRNA in CIHP-1 cells; (c) relative expression of EGR1 mRNA in CIHP-1 cells; (d) western blot analysis results of VDR and EGR1 in CIHP-1 cells; (e) relative expression of miR-675 in HEK 293 cells; (f) relative expression of VDR mRNA in HEK 293 cells; (g) Relative expression of EGR1 mRNA in HEK 293 cells; (h) western blot analysis results of VDR and EGR1 in HEK 293 cells. EGR1: early growth response protein 1; miR-675: microRNA-675; mRNA: messenger RNA; NC: negative control; VDR: vitamin D receptor
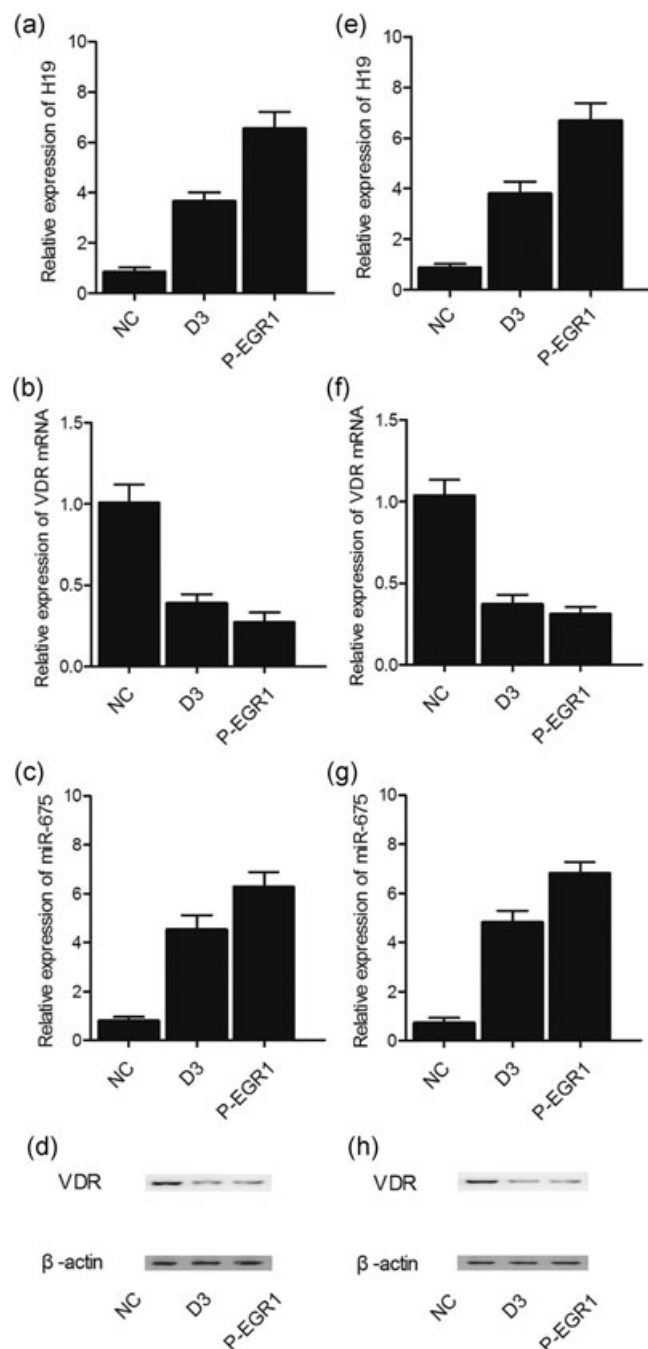
FIGURE 2 Expression levels of miR-675, H19, and VDR in CIHP-1 cells and HEK 293 cells treated with $1,25D_3$ or EGR1. (a) Relative expression of H19 in CIHP-1 cells; (b) relative expression of miR-675 in CIHP-1 cells; (c) relative expression of VDR mRNA in CIHP-1 cells; (d) western blot analysis results of VDR in CIHP-1 cells; (e) relative expression of H19 in HEK 293 cells; (f) relative expression of miR-675 in HEK 293 cells; (g) relative expression of VDR mRNA in HEK 293 cells; (h) western blot analysis results of VDR in HEK 293 cells. $1,25D_3$: 1,25-dihydroxyvitamin D3; EGR1: early growth response protein 1; miR-675: microRNA-675; mRNA: messenger RNA; NC: negative control; VDR: vitamin D receptor

is a target gene of miR-675 (Figure 3a). To verify the above hypothesis, luciferase activities were detected in CIHP-1 or HEK 293 cells treated with miR-675 mimics or H19 following the transfection of wild-type/mutant VDR. As shown in Figure 3b, the relative luciferase activity of wild-type VDR was obviously reduced in CIHP-1 cells treated with miR-675 mimics. Meanwhile, the relative luciferase activity of mutant VDR only showed slight changes. In addition, the relative luciferase activity of wild-type VDR decreased in the presence of H19, whereas the presence of H19 did not affect the luciferase activity of mutant VDR (Figure 3d). Furthermore, similar results were obtained in HEK 293 cells (Figure 3c,e) validating VDR as a target of miR-625.

3.4 | EGR1 positively regulated the expression of H19

We also established three treatment groups using CIHP-1 and HEK 293 cells: an H19 promoter treatment group, an H19 promoter + EGR1 treatment group, and a blank control group. As shown in Figure 4a, the luciferase activity of CIHP-1 cells treated with H19 promoters was evidently increased compared with that in the blank control group. However, when CIHP-1 cells were treated with both H19 promoter and EGR1, the luciferase activity was further increased. Because similar results were obtained using HEK 293 cells, a positive regulatory relationship between EGR1 and H19 was established (Figure 4b).

3.5 | Expression of H19/miR-675/VDR/EGR1 in clinical samples

Fifty-four DM patients were recruited into this study. In addition, the presence of DN was utilized as an indicator to divide the patients into a DN(+) group (N = 29) and a DN(−) group (N = 25). The relative expression of relevant factors involved in the pathological mechanism of DN was measured using qRT-PCR. As shown in Figure 5, the relative expression of both H19 (Figure 5a) and miR-625 (Figure 5b) significantly increased in the DN(+) group compared with that in the DN(−) group. On the other hand, the relative expression of VDR mRNA and EGR1 mRNA sharply decreased in the DN(+) group. The differential expression of VDR and EGR1 in the DN(+) and DN(−) groups was further verified via IHC assays. As shown in Figure 6, the expression of VDR was suppressed in the DN(+) group compared with that in the DN(−) group.

3.6 | A negative feedback loop was established among H19, miR-675, VDR, and EGR1

Altogether, the results presented in this study indicated the presence of a negative feedback loop in the pathological mechanism of DN (Figure 7). In this negative feedback loop, H19 negatively regulates
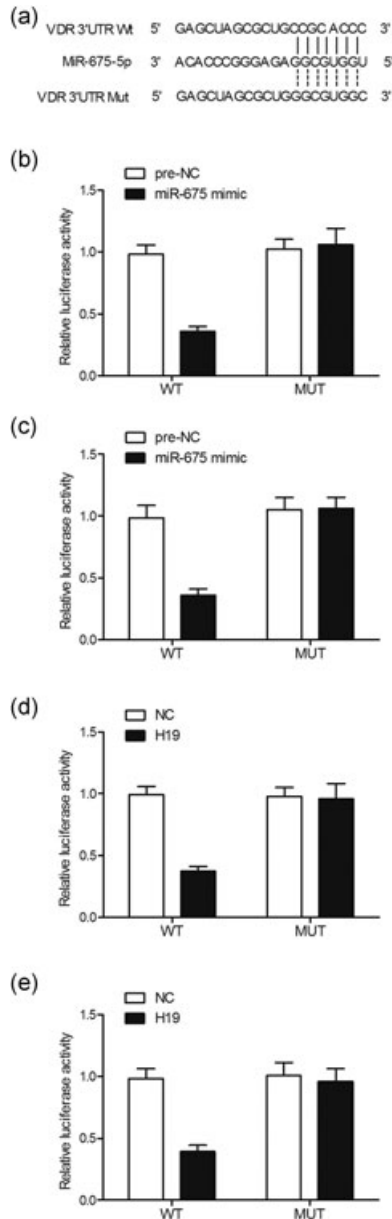
FIGURE 3 Luciferase activity of VDR in CIHP-1/HEK 293 cells. (a) VDR is a potential target gene of miR-675; (b) relative luciferase activity of wild-type/mutant VDR in CIHP-1 cells cotransfected with miR-675 mimics; (c) relative luciferase activity of wild-type/mutant VDR in HEK 293 cells cotransfected with miR-675 mimics; (d) relative luciferase activity of wild-type/mutant VDR in CIHP-1 cells cotransfected with H19 mimics; (e) relative luciferase activity of wild-type/mutant VDR in HEK 293 cells cotransfected with H19 mimics. miR-675: microRNA-675; NC: negative control; VDR: vitamin D receptor
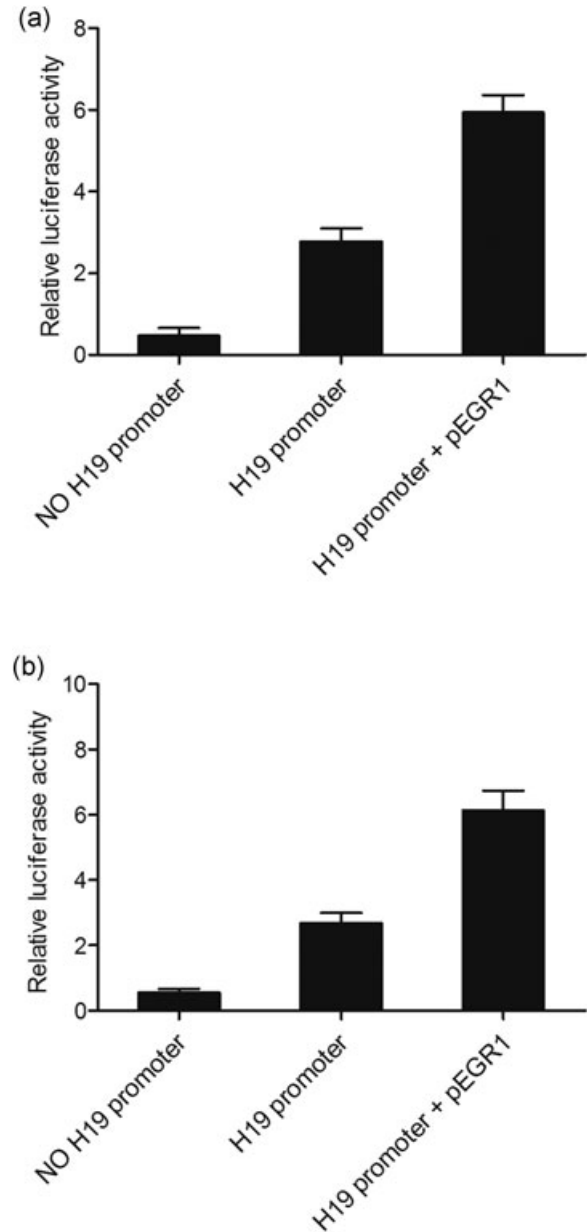

FIGURE 4 Luciferase activity in CIHP-1/HEK 293 cells. (a) Luciferase activity of CIHP-1 cells cotransfected with H19 promoter or H19 promoter + EGR1. (b) Luciferase activity of HEK 293 cells cotransfected with H19 promoter or H19 promoter + EGR1. EGR1: early growth response protein 1

the expression of VDR by upregulating the expression of miR-675. The reduced VDR expression leads to the downregulation of EGR1 expression. As EGR1 is positively related to H19, the downregulation of EGR1 also inhibits the expression of H19. As the negative feedback loop lowered the VDR expression, it is necessary to maintain the homeostasis of VDR and to reduce the incidence of DN in the body.

4 | DISCUSSION

It has been confirmed recently that miR-675 could alter the epigenetic modifications in histone by reducing HP1α (Dey et al., 2014). Indeed, miR-675 increased the occupancy of EGR1 on the imprinting control region of H19, thus eventually increasing H19 expression. These results suggested that HP1α, an isoform of HP1, could act as a hub during the epigenetic regulation of the miR-675 action (Dey et al., 2014). Furthermore, it was demonstrated that H19 expression is significantly increased in cells coexpressing EGR1 and miR-675, indicating that miR-675 could increase H19 expression by elevating the occupancy of
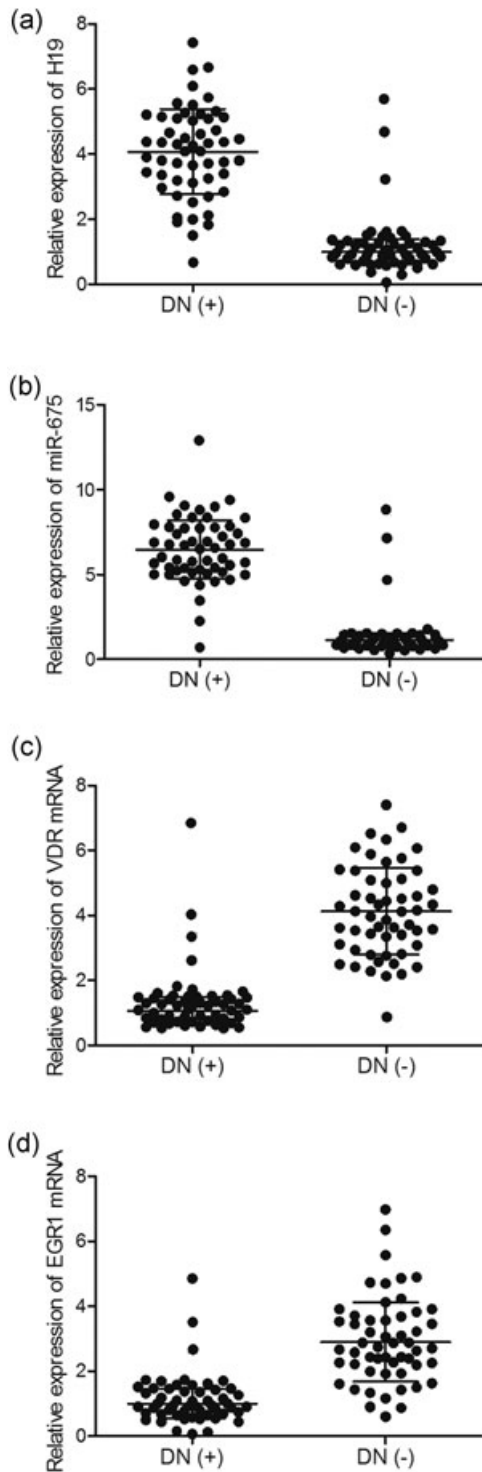
FIGURE 5 Differentiated expression of H19/miR-675/VDR/
EGR1 in DM patients with or without DN. (a) Relative
expression of H19 in DM patients with or without DN;
(b) relative expression of miR-675 in DM patients with or without
DN; (c) relative expression of VDR mRNA in DM patients with or
without DN; (d) relative expression of EGR1 mRNA in DM patients
with or without DN. DM: diabetes mellitus; DN: diabetic
nephropathy; EGR1: early growth response protein 1;
miR-675: microRNA-675; mRNA: messenger RNA; VDR: vitamin D
receptor

EGR1 on the imprinting control region of H19 (Dey et al., 2014). In this
study, a computational analysis was utilized to identify VDR as a target
gene of miR-675. This result was then confirmed by the luciferase assay.
In addition, using the luciferase assay, we confirmed the stimulatory
effect of EGRs on the promoter of H19. Furthermore, we examined the
effect of vitamin D3 and EGR1 on the expression of H19 and
miR-675 and found that the relative expression of H19 and miR-675
was upregulated in the presence of $1,25D_3$ and EGR1, whereas the
expression of VDR was suppressed in the presence of $1,25D_3$ and
EGR1. The above results established a potential negative feedback loop
among H19, miR-675, VDR, and EGR1. On the basis of the above-
mentioned data as well as the results of our literature research, we
hypothesized that the negative feedback loop of H19, miR-675, VDR,
and EGR1 is required to maintain the homeostasis of VDR.

As a member of the nuclear receptor family, VDR acts as a
transcription factor that can be induced by ligands (Chambon, 1996). In
fact, the binding of $1,25D_3$ to VDR can induce a conformational change
in the VDR. Whereas the direct regulation of VDR expression relies on
the function of VD-responsive elements (VDRE) in the promoters of its
target genes, some genes controlled by $1,25D_3$ do not have VDRE in
their promoters. Therefore, VDR does not seem to regulate gene
expression by interacting with VDRE in the promoter of its target genes.
In fact, VDR seems to control gene expression by interacting with
multiple transcription factors including β-catenin/TCF and Sp1 (Palmer
et al., 2001; Szpirer et al., 1991). Furthermore, VD analogs were reported
to inhibit the activation of the Wnt/β-catenin signaling pathway in
podocytes, thus ameliorating podocyte impairment (He, Kang, Dai, & Liu,
2011). Although the baseline expression of VDR in podocytes is often
low, VDR expression in podocytes can be induced by $1,25D_3$ (Deb et al.,
2011). It has been shown that $1,25D_3$ treatment of podocytes could
reduce the severity of albuminuria and prevent podocyte damage in
adriamycin-induced nephropathy, puromycin aminonucleoside-induced
podocyte apoptosis, and nephrectomized rats (Deb et al., 2011; He et al.,
2011; Kuhlmann et al., 2004; Xiao et al., 2009). It has also been shown
that when doxercalciferol, a VD analog, was administered at a low dose,
it could prevent albuminuria and significantly attenuated the apoptosis of
podocytes. However, the VD analog showed no effect on the
development of DN in wild-type mice (Wang et al., 2012). In addition
to its role in maintaining phosphate and calcium homeostasis, VD is also
known to play a significant proapoptotic, prodifferentiation, and
antiproliferative role in a wide range of tissue and cell types such as in
tumor cells (Thorne & Campbell, 2008). In addition, as a metabolite of
VD, $1,25D_3$ can bind to VDR and facilitate the translocation of the VDR-
ligand complex into the nucleus. In the nucleus, the VDR-ligand complex
binds to the VDRE in target genes (Bikle, 2011). It has been shown that
the loss of VDR in human prostate cancer and breast cancer could
induces cell apoptosis by suppressing the function of the Wnt/β-catenin
signaling (Zheng et al., 2017).

The results obtained in this study indicated the presence of a
negative feedback loop in the pathological mechanism of DN, and
such a negative feedback loop is required to maintain the home-
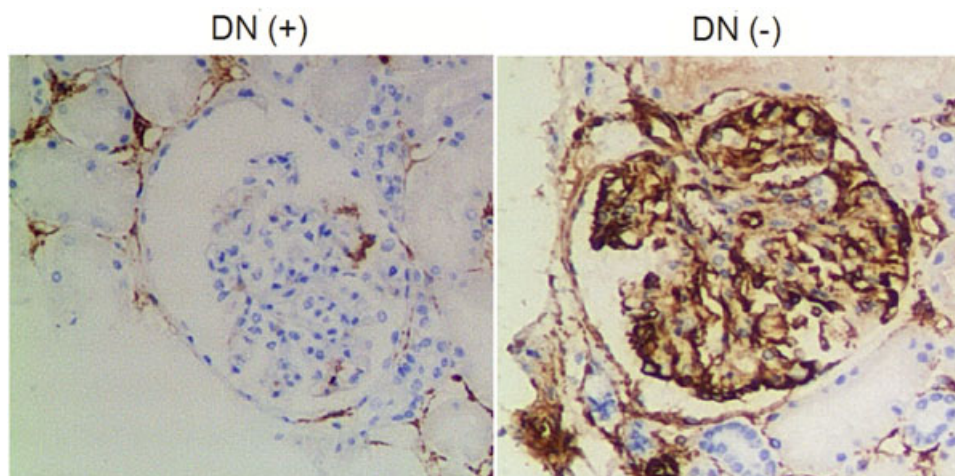ostasis of VDR and to reduce the incidence of DN.

FIGURE 6   IHC assay of VDR in DM patients with or without DN. DM: diabetes mellitus; DN: diabetic nephropathy; IHC: immunohistochemistry; VDR: vitamin D receptor [Color figure can be viewed at wileyonlinelibrary.com]
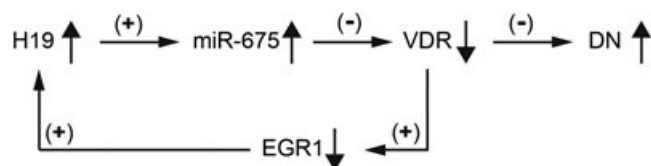

FIGURE 7   Negative feedback loop of H19, miR-675, VDR and EGR1. DN: diabetic nephropathy; EGR1: early growth response protein 1; miR-675: microRNA-675; VDR: vitamin D receptor

We have noticed that VDR's roles in different pathological processes might not always be consistent and sometimes might be conflicting such as its role in the pathogenesis of DN and its role in tumorigenesis. We reasoned that such a discrepancy might be attributed to the difference of its downstream signaling pathways as well as the complicated interaction network of the intracellular signal transduction.

5 | CONCLUSION

In summary, we first suggested that a negative feedback loop of H19/miR-675/EGR1 is involved in the development of DN. We found that miR-675 is located within the chromosome segment of H19, while the increase in H19 expression also upregulated the expression of both miR-675-5p and miR-675-3p. Furthermore, VDR was reported as a target gene of miR-675 in human cells, while the activation of the VD signaling pathway could promote the expression of EGR1, a transcription factor of H19. VDR plays an important role in podocyte apoptosis and DN. Therefore, H19 may serve as a novel biomarker for DN.

CONFLICT OF INTERESTS

The authors declare that there are no conflict of interests.

AUTHOR CONTRIBUTIONS

Study director: Y. Z. P.; Study plan: W. X. F. and Y. Z. P.; Literature collection: Y. N. Y. and J. Z.; Data collection: W. X. F., Z. L., Y. N. Y., and J. Z.; Data analysis: Z. L., Y. N. Y., and J. Z.; Data interpretation: W. X. F., Y. Z. P., and Z. L.; Manuscript draft: W. X. F. and Z. L.; Manuscript improvement: Y. Z. P.; All authors read and approved the final manuscript.

ORCID

YunZhu Peng http://orcid.org/0000-0003-1908-987X

REFERENCES

Allen, D. A., Harwood, S., Varagunam, M., Raftery, M. J., & Yaqoob, M. M. (2003). High glucose-induced oxidative stress causes apoptosis in proximal tubular epithelial cells and is mediated by multiple caspases. *FASEB Journal, 17,* 908–910.

Bartolomei, M. S., Zemel, S., & Tilghman, S. M. (1991). Parental imprinting of the mouse H19 gene. *Nature, 351,* 153–155.

Bikle, D. D. (2011). Vitamin D: An ancient hormone. *Experimental Dermatology, 20,* 7–13.

Cai, X., & Cullen, B. R. (2007). The imprinted H19 noncoding RNA is a primary microRNA precursor. *RNA, 13,* 313–316.

Chambon, P. (1996). A decade of molecular biology of retinoic acid receptors. *FASEB Journal, 10,* 940–954.

Chen, S., Bu, D., Ma, Y., Zhu, J., Chen, G., Sun, L., ... Wang, P. (2017). H19 overexpression induces resistance to 1,25(OH)2D3 by targeting VDR through miR-675-5p in colon cancer cells. *Neoplasia, 19,* 226–236.

Clark, M. B., Amaral, P. P., Schlesinger, F. J., Dinger, M. E., Taft, R. J., Rinn, J. L., ... Mattick, J. S. (2011). The reality of pervasive transcription. *PLOS Biology, 9,* e1000625.

Danilenko, M., Wang, X., & Studzinski, G. P. (2001). Carnosic acid and promotion of monocytic differentiation of HL60-G cells initiated by other agents. *Journal of the National Cancer Institute, 93,* 1224–1233.

Deb, D. K., Wang, Y., Zhang, Z., Nie, H., Huang, X., Yuan, Z., ... Li, Y. C. (2011). Molecular mechanism underlying 1,25-dihydroxyvitamin D regulation of nephrin gene expression. *Journal of Biological Chemistry*, *286*, 32011–32017.

Dey, B. K., Pfeifer, K., & Dutta, A. (2014). The H19 long noncoding RNA gives rise to microRNAs miR-675-3p and miR-675-5p to promote skeletal muscle differentiation and regeneration. *Genes and Development*, *28*, 491–501.

Friedman, S., Jones, H. W., 3rd, Golbetz, H. V., Lee, J. A., Little, H. L., & Myers, B. D. (1983). Myers BD: Mechanisms of proteinuria in diabetic nephropathy. II. A study of the size-selective glomerular filtration barrier. *Diabetes*, *32*(Suppl 2), 40–46.

He, W., Kang, Y. S., Dai, C., & Liu, Y. (2011). Blockade of Wnt/beta-catenin signaling by paricalcitol ameliorates proteinuria and kidney injury. *Journal of the American Society of Nephrology*, *22*, 90–103.

Jensen, H. A., Yourish, H. B., Bunaciu, R. P., Varner, J. D., & Yen, A. (2015). Induced myelomonocytic differentiation in leukemia cells is accompanied by noncanonical transcription factor expression. *FEBS Open Bio*, *5*, 789–800.

Jiang, Y. J., & Bikle, D. D. (2014). LncRNA profiling reveals new mechanism for VDR protection against skin cancer formation. *Journal of Steroid Biochemistry and Molecular Biology*, *144*, 87–90.

Kuhlmann, A., Haas, C. S., Gross, M. L., Reulbach, U., Holzinger, M., Schwarz, U., ... Amann, K. (2004). 1,25-Dihydroxyvitamin D3 decreases podocyte loss and podocyte hypertrophy in the subtotally nephrectomized rat. *American Journal of Physiology. Renal Physiology*, *286*, F526–F533.

Li, G., Li, Y., Liu, S., Shi, Y., Chi, Y., Liu, G., & Shan, T. (2013). Gremlin aggravates hyperglycemia-induced podocyte injury by a TGFbeta/ smad dependent signaling pathway. *Journal of Cellular Biochemistry*, *114*, 2101–2113.

Li, H., Li, J., Jia, S., Wu, M., An, J., Zheng, Q., ... Lu, D. (2015). miR675 upregulates long noncoding RNA H19 through activating EGR1 in human liver cancer. *Oncotarget*, *6*, 31958–31984.

Li, X., Wang, H., Yao, B., Xu, W., Chen, J., & Zhou, X. (2016). lncRNA H19/ miR-675 axis regulates cardiomyocyte apoptosis by targeting VDAC1 in diabetic cardiomyopathy. *Scientific Reports*, *6*, 36340.

Lippert, J., Ritz, E., Schwarzbeck, A., & Schneider, P. (1995). The rising tide of endstage renal failure from diabetic nephropathy type II—an epidemiological analysis. *Nephrology, Dialysis, Transplantation*, *10*, 462–467.

Menini, S., Iacobini, C., Oddi, G., Ricci, C., Simonelli, P., Fallucca, S., ... Pugliese, G. (2007). Increased glomerular cell (podocyte) apoptosis in rats with streptozotocin-induced diabetes mellitus: Role in the development of diabetic glomerular disease. *Diabetologia*, *50*, 2591–2599.

Moreno-Moya, J. M., Vilella, F., & Simón, C. (2014). MicroRNA: Key gene expression regulators. *Fertility and Sterility*, *101*, 1516–1523.

Perkel, J. M. (2013). Visiting "noncodarnia". *Biotechniques*, *54*(301), 303–304.

Pálmer, H. G., González-Sancho, J. M., Espada, J., Berciano, M. T., Puig, I., Baulida, J., ... Muñoz, A. (2001). Vitamin D(3) promotes the differentiation of colon carcinoma cells by the induction of E-cadherin and the inhibition of beta-catenin signaling. *Journal of Cell Biology*, *154*, 369–387.

Remuzzi, G., Schieppati, A., & Ruggenenti, P. (2002). Clinical practice. Nephropathy in patients with type 2 diabetes. *New England Journal of Medicine*, *346*, 1145–1151.

Rönnau, C. G. H., Verhaegh, G. W., Luna-Velez, M. V., & Schalken, J. A. (2014). Noncoding RNAs as novel biomarkers in prostate cancer. *BioMed Research International*, *2014*, 591703–591717.

Salmena, L., Poliseno, L., Tay, Y., Kats, L., & Pandolfi, P. P. (2011). A ceRNA hypothesis: The Rosetta Stone of a hidden RNA language? *Cell*, *146*, 353–358.

Szpirer, J., Szpirer, C., Riviere, M., Levan, G., Marynen, P., Cassiman, J. J., ... DeLuca, H. F. (1991). The Sp1 transcription factor gene (SP1) and the 1,25-dihydroxyvitamin D3 receptor gene (VDR) are colocalized on human chromosome arm 12q and rat chromosome 7. *Genomics*, *11*, 168–173.

Tanaka, E., Asanuma, K., Kim, E., Sasaki, Y., Trejo, J. A. O., Seki, T., ... Tomino, Y. (2014). Notch2 activation ameliorates nephrosis. *Nature Communications*, *5*, 3296.

Thorne, J., & Campbell, M. J. (2008). The vitamin D receptor in cancer. *Proceedings of the Nutrition Society*, *67*, 115–127.

Tsang, W. P., Ng, E. K. O., Ng, S. S. M., Jin, H., Yu, J., Sung, J. J. Y., & Kwok, T. T. (2010). Oncofetal H19-derived miR-675 regulates tumor suppressor RB in human colorectal cancer. *Carcinogenesis*, *31*, 350–358.

Valdivielso, J. M. (2009). The physiology of vitamin D receptor activation. *Contributions to Nephrology*, *163*, 206–212.

Wang, Y., Deb, D. K., Zhang, Z., Sun, T., Liu, W., Yoon, D., ... Li, Y. C. (2012). Vitamin D receptor signaling in podocytes protects against diabetic nephropathy. *Journal of the American Society of Nephrology*, *23*, 1977–1986.

Wild, S., Roglic, G., Green, A., Sicree, R., & King, H. (2004). Global prevalence of diabetes: Estimates for the year 2000 and projections for 2030. *Diabetes Care*, *27*, 1047–1053.

Xiao, H., Shi, W., Liu, S., Wang, W., Zhang, B., Zhang, Y., ... Liang, Y. (2009). 1,25-Dihydroxyvitamin D(3) prevents puromycin aminonucleoside-induced apoptosis of glomerular podocytes by activating the phosphatidylinositol 3-kinase/Akt-signaling pathway. *American Journal of Nephrology*, *30*, 34–43.

Zhang, Z., Sun, L., Wang, Y., Ning, G., Minto, A. W., Kong, J., ... Li, Y. C. (2008). Renoprotective role of the vitamin D receptor in diabetic nephropathy. *Kidney International*, *73*, 163–171.

Zhang, Z., Zhang, Y., Ning, G., Deb, D. K., Kong, J., & Li, Y. C. (2008). Combination therapy with AT1 blocker and vitamin D analog markedly ameliorates diabetic nephropathy: Blockade of compensatory renin increase. *Proceedings of the National Academy of Sciences of the United States of America*, *105*, 15896–15901.

Zheng, Y., Trivedi, T., Lin, R. C., Fong-Yee, C., Nolte, R., Manibo, J., ... Seibel, M. J. (2017). Loss of the vitamin D receptor in human breast and prostate cancers strongly induces cell apoptosis through downregulation of Wnt/beta-catenin signaling. *Bone Research*, *5*, 17023.